International Journal of Basic and Applied Sciences, 14 (3) (2025) 206-215

International Journal of Basic and Applied Sciences

Website: www.sciencepubco.com/index.php/IJBAS
https://doi.org/10.14419/3rgs0w03
Research paper



Fractal Revolution: Unleashing Multi-Band Power in Compact Patch Antennas for 5G and Beyond

Sudhir Kadam [1], Harshada Mhetre [1] *, Prasad Kadam [2], Vishal Patil [3], Sachin Gurav [4], Snehal Mane [2], Sagar Sutar [5]

[1] Department of Electronics and Communication Engineering, Bharati Vidyapeeth (Deemed to be University) College of Engineering, Pune, Maharashtra, India.
[2] Department of Electronics and Communication Engineering, Bharati Vidyapeeth (Deemed to be University) College of Engineering, Pu-ne, Maharashtra, India.
[3] Department of Computer Science Engineering, MIT School of Computing, MIT ADT University, Pune, Maharashtra, India.
[4] Sharad Institute of Technology College of Engineering, Yadrav, Maharashtra, India.
[5] Department of Electronics Engineering, Bharati Vidyapeeth (Deemed to be University) College of Engineering, Pune-Satara, Pune, Ma-harashtra, India
**Corresponding author E-mail: hvmhetre@bvucoep.edu.in*

Received: June 4, 2025, Accepted: July 4, 2025, Published: July 21, 2025

Abstract

This research presents the design and performance analysis of a dual-band microstrip patch antenna for wireless applications. The antenna, fabricated on an FR-4 substrate, incorporates space-filling and self-similar properties to enhance performance. It operates in multiple frequency bands (2.2571 GHz, 3.8571 GHz, 5.0000 GHz, and 7.1714 GHz) with return loss values below -9 dB, indicating good impedance matching. Simulation results demonstrate high radiation efficiency, stable group delay, and consistent radiation patterns across the operating bands. The antenna's peak gain exceeds 5 dB over a broad frequency range, occasionally reaching 8 dB. These characteristics make it suitable for various wireless applications, including WLAN, WiMAX, and sub-6 GHz 5G systems. The study concludes that the designed antenna exhibits strong multiband performance with stable and efficient operation over the 2.2-7.1 GHz frequency band, making it viable for integration in high-performance RF systems.

Keywords: *Dielectric Substrates; Microstrip Antenna*; *Multi-Band; Patch Geometry; Wireless Communication*

1. Introduction

1.1 Background and motivation

This study aims to advance the development of antennas with enhanced performance characteristics suitable for modern wireless communication systems. Specifically, it investigates multiband patch antenna configurations that have shown significant advantages over conventional antenna designs. The primary objective of this study was to integrate the desirable functional attributes and ensure efficient electromagnetic energy radiation.

- By optimizing their form to increase their electrical length, the overall size of the antenna is reduced.
- Antennas' total size is reduced by optimizing their shape to increase electrical length.
- Multiband antennas are advantageous for utilizing the Patch

1.2 Literature survey

Dual-band patch antenna geometries often leverage space-filling and self-similar properties to enhance performance. Antennas function as transducers that transmit and receive electromagnetic energy, and their design involves optimizing a trade-off among key parameters, such as efficiency, gain, physical size, and operational bandwidth. Traditional antenna structures are predominantly based on Euclidean geometries, where the enclosed area scales proportionally with the square of linear dimensions. For instance, tripling the side length of a Euclidean square results in a nine-fold increase in the enclosed area. However, Euclidean-based antenna designs are limited in performance, as they tend to exhibit high quality (Q) factors and reduced efficiency when miniaturized, making them less suitable for compact and high-performance applications [1]. Contemporary wireless communication devices are becoming increasingly prevalent and operate across a broad spectrum of frequencies. These devices are characterized by their compact size, low profile, multi-band capabilities, high dielectric

Copyright © Sudhir Kadam et al. This is an open access article distributed under the Creative Commons Attribution License, which permits unrestricted use, distribution, and reproduction in any medium, provided the original work is properly cited.

substrates, extensive electrical length, and other highly desirable attributes[2]. . The reduction in bandwidth, coupled with constraints in manufacturing and materials, may present significant production challenges for extremely narrow-band components, such as microstrip patches. Consequently, broadband elements with minimal or no dielectric loading are advantageous. Substantial evidence supports the belief that the multiband operation of the patch antenna is attributable to either its space-filling or self-similar structure [3].
The proposed microstrip antenna, incorporating a defective ground structure (DGS) based on a complementary split-ring resonator (CSRR) array, was developed for Wi-MAX applications at a frequency of 2.6 GHz. The antennas were fabricated using a 1.6 mm-thick FR-4 substrate with a dielectric constant (εr) of 4.4. The physical dimensions of the proposed antenna are equivalent to those of a single CSRR-structured microstrip antenna with a resonance frequency of 3.5 GHz [3]. An antenna prototype was constructed using a cost-effective FR-4 glass epoxy substrate. The proposed antenna was compact and had a bandwidth of 700 MHz. It is capable of covering 5G NR sub-6GHz wireless application bands [4].
The utilization of multiband patch geometry, which is a variant of non-Euclidean geometry, in small Euclidean antennas can effectively resolve these challenges. It is noteworthy that the radiation resistance (Rr) is consistently greater for island or patch loop antennas than for small [5] loop antennas of equivalent dimensions. The radiation resistance (Rr) of a patch antenna decreases as a function of the compression of its perimeter (C). Consequently, multiband patch antennas demonstrate superior performance over Euclidean designs when compact sizes are required [2]. Patch geometry can be categorized into current technological advancements encompassing the Internet, cellular telecommunications, and the increasing demand from individual users for wireless access to devices such as pagers, cell phones, the Internet, and personal digital assistants[5]. Meanwhile, competing wireless broadband technologies such as GSM, TDMA, and CDMA are being promoted by wireless manufacturers in today's market [6]. Considering the aforementioned, it is clear that an antenna system that facilitates effective access to the Internet, mobile phones, pagers, PDAs, radio, and/or similar devices is needed in the field of technology. In other words, a multiband patch antenna is required in the state-of-the-art [7]. The polarization of an antenna is a critical parameter that must be considered a determining factor in the application-oriented electronics market. Antennas operating within the same frequency band, but exhibiting different polarizations, can be utilized concurrently. It is possible to conduct studies on the proposed antennas concerning this aspect of polarization. These antennas were tested in a controlled laboratory environment; however, the influence of external factors such as dust, dew, rain, and temperature is also crucial for the successful deployment of these antennas under field conditions[4]. Concurrently, wireless broadband technologies such as GSM, TDMA, and CDMA are being advanced by wireless manufacturers in the current market [8]. In light of the aforementioned, it is evident that an antenna system facilitating effective access to the Internet, mobile phones, pagers, PDAs, radio, and similar devices is essential in the technological domain. In other words, state-of-the-art multiband patch antennas are required [9]. The polarization of an antenna is a critical parameter that must be considered a determining factor in the application-oriented electronics market. Antennas operating within the same frequency band, but exhibiting different polarizations, can be utilized concurrently. It is feasible to conduct studies on the proposed antennas concerning this aspect of polarization. These antennas were tested in a controlled laboratory environment; however, the influence of external factors such as dust, dew, rain, and temperature is also crucial for the successful deployment of these antennas under field conditions.[6] [10]

1.3 Research gap

Despite the considerable advancements in multiband patch antenna design, current literature often isolates performance parameters—such as gain, bandwidth, or miniaturization—without offering a comprehensive design that successfully balances all key attributes. Additionally, many studies neglect real-world deployment conditions, where temperature fluctuations, humidity, and mechanical stress can affect performance. Moreover, while the benefits of unconventional geometries are known, systematic frameworks for their integration into practical antenna models remain underdeveloped.[1] [11]

1.4 Purpose of the study

This research seeks to address the identified gaps by developing a multiband patch antenna that harmonizes compactness, operational efficiency, and real-world applicability. The objective is to construct a design using CSRR-based DGS on an FR-4 substrate, targeting WiMAX and sub-6GHz 5G applications. The antenna aims to exhibit wide bandwidth, reliable radiation characteristics, and resilience to environmental stressors, making it suitable for integration into modern wireless systems.

2. Patch antenna

2.1 Dual-band patch antenna

This type of microstrip patch antenna is employed in applications that involve many bands. The dual-band patch could have self-similar geometric patterns that could build nearly any complex structure seen in nature by repeatedly creating certain fundamental geometries. Dual-band patch antennas use patch geometry. This increases the perimeter of the material to improve the overall electrical length of the antenna. The total surface area or volume remains constant [2] [9]. Patch antennas are sometimes called space-filling curves or multilayer curves, but what makes them unique is the way they repeat a pattern across two or more scale levels, or "iterations." Therefore, dual-band patch antennas are incredibly small, multiband, or wideband, and have practical applications in microwave and cellular communications [3] in Figure 2.

Table 1: Comparator of Feed

Characte-ristics	Microstrip Line Feed	Coaxial feed	Aperture-coupled feed	Proximity-coupled feed	Novelty of the research
Spurious feed radiation	High	High	Low	Low	Minimum
Reliability	Better	Poor due to soldering	Acceptable	Acceptable	Good
Ease of fabrication	Relatively easy	Soldering and drilling are needed	Alignment re-quired	Alignment re-quired	Alignment is required
Impedance matching	Easy	Easy	Easy	Easy	Easy
Bandwidth	2-5%	2-5%	2-5%	9-11%	13%

Table 1 shows that the parameters carried out under the novelty of the research are in an enhanced state when verified with other research contributions pertaining to spurious feed radiation, Reliability, Ease of fabrication, impedance matching, and bandwidth.
The dielectric substrate of a microstrip patch antenna has a ground plane on one side and a radiating patch on the other, as shown in Figure 1. Typically, a patch is composed of conductive materials, such as copper or gold, and can take on any form. The radiating patch and feed lines are typically photoetched on a dielectric substrate[12].

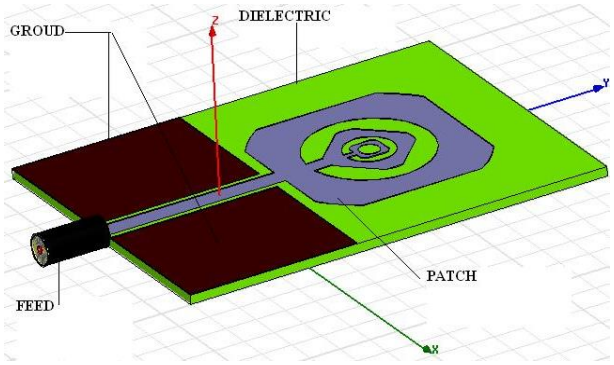


Fig.1: Dielectric Substrate.

2.2 Compact dimensions

This is quite small in size. The primary benefit of this antenna is its ability to adhere to a surface, conserving more room, and its self-similarity, which also makes it appealing. [13] It is small with high to exceptional efficiency and gains compared to antennas with traditional designs, as shown in Figure 3.

2.3 Space-filling property

Because the same antenna size may be used in a system operating in various bands, it makes effective use of the available space. It is small and has excellent efficiencies and gains. [4] as shown in Figure 3.

2.4 Mechanical simplicity and robustness

The dual-band patch antenna shape, not the inclusion of discrete components, is responsible for its features. We can stick it on any surface, which makes it useful for applications such as space satellites, [14] as shown in Figure 3.

2.5 Similarity to oneself

Dual-band patch antennas have the advantage of being extremely easy to design, such as the application of a basic form through several iterations, which results in a high efficiency, multiband nature, and other benefits.[8]

3. Materials and methods

3.1 Development multiband patch antenna

The formation of a dual-band patch antenna can be envisioned in a variety of ways. To construct a dual-band patch,a smaller self-similar entity is created as a result of this process. The ability to create smaller pieces without compromising the efficiency or bandwidth makes this technique appealing.[3]

3.2 Methods of multiband patch antenna design

The geometries that are repeatedly created can be used in two different ways. By using Patch's capacity to fill available space and squeeze long electrical lengths into tiny physical volumes, antennas may be made smaller.
The second approach designs antennas with comparable characteristics at different frequency bands that correlate to the scaled geometry by utilizing different scales of the self-similar geometry. This idea results in an antenna that appears physically the same or very similar across a range of frequency bands [1] [5] [8].

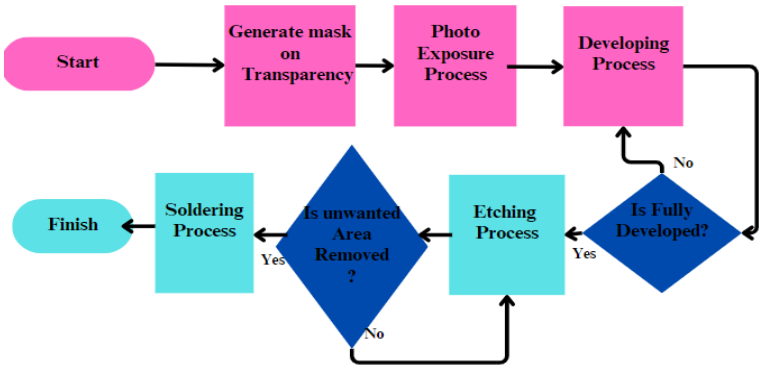


Fig.2: Multiband Patch Antenna &Properties of Dual Band Patch Antenna.

3.3 Design of multiband patch antenna

As shown in Figure 3, a rectangular patch measuring 30 mm × 30 mm was used to form the radiating antenna. This patch was placed on a rectangular FR4 substrate measuring 48 mm × 65 mm with a substrate thickness of 1.53 mm and a relative permittivity of 4.4. Next, the edges of this fundamental structure—a square—are bent by crossing paths with an 18-mm-radius cylinder, the center of which is the centroid of the square. A curved edge aids in optimizing the bandwidth use. The center portion of a 10-mm-long cylindrical form was etched out. This is the core structure, which is then rotated by 45 °and scaled down to 40% for each patch step before it. Three of these Patches were joined together, and a 3.1 mm-wide feed line was attached to it. The level surface on both sides of the feed was 22.5 mm x 28 mm. The gap between the ground and feed was 0.95 mm, mmand ground to a patch 0.22 mm.[12]

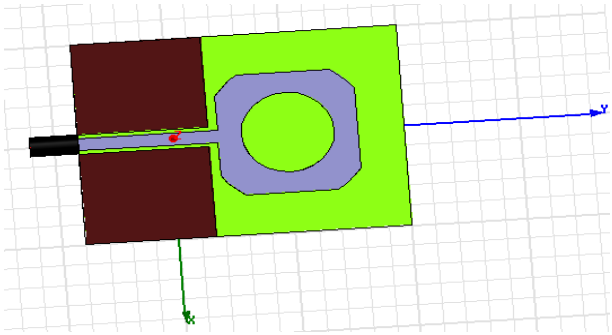


Fig.3: Stage 1.

The proposed structure is a microstrip patch antenna configured on a rectangular substrate, as described in Stage 1(Fig.3). A circular ring resonator is etched on the radiating patch to improve performance characteristics such as bandwidth and miniaturization. The antenna was excited through a microstrip feed line connected to the resonator and protruding from the coaxial port. A partial ground plane or absorber boundary is positioned on the other side of the substrate to aid impedance matching and minimize back radiation. The entire geometry was simulated in a specified coordinate system for a precise electromagnetic analysis. [2] [6] [12].

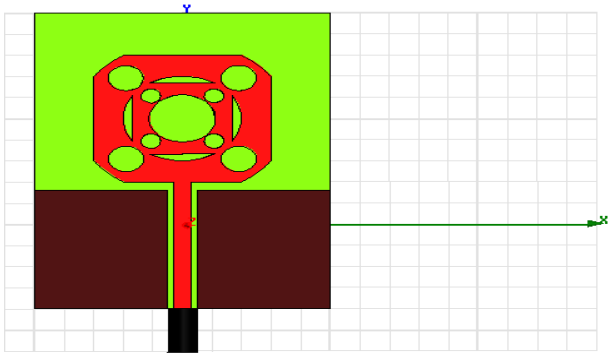


Fig. 4: Stage 2.

The antenna design shown in stage 2 (Fig. 4) has a complex metamaterial-inspired radiating patch on a rectangular substrate. The red radiating structure is a central circular patch surrounded by several symmetrically located circular slots and split-ring resonators to create multi-band or wideband functionality. A microstrip feed line was used to excite the antenna, running from a coaxial port along the bottom center of the board. The bottom part of the substrate contained a partial ground plane, as indicated by dark brown, to improve the impedance matching and radiation efficiency. The antenna geometry was examined in a Cartesian coordinate system to determine the correct electro-magnetic performance prediction.[7] [14].

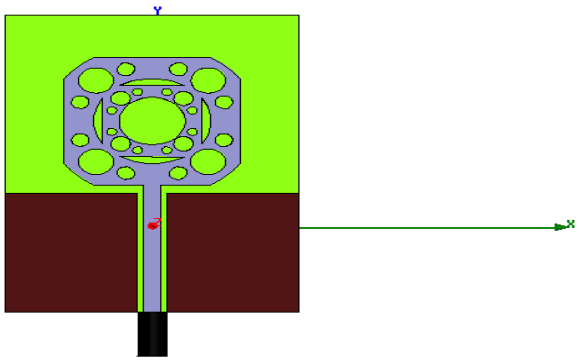


Fig. 5: Stage 3.

The antenna structure shown in Stage 3 (Fig. 5) exhibits a metamaterial-driven microstrip patch coupled with a number of asymmetrically located concentric circular slot rings and circular etchings. This etched structure appears on a green dielectric substrate and is proposed to improve the resonant properties of the antenna for multi-band or ultra-wideband (UWB) performance. The feed system comprises a microstrip line to which a coaxial port at the bottom center is joined, allowing good excitation of the radiating structure. A partial ground plane was installed at the bottom to achieve better impedance matching and suppress the effects of surface waves. The design was simulated using the Cartesian coordinate system (X-Y axes) to ascertain an accurate electromagnetic field analysis and evaluate the radiation performance effectively.[12].

4. Experimental & Simulated Results

The experimental and simulated results are as follows in the number of sections,

4.1 VSWR

The graph shows the simulated reflection coefficient (S_{11}) response of the given structure over a frequency range of 0–12 GHz, as obtained from ANSYS HFSS. The graph depicts the magnitude of S_{11} in decibels (dB), which is the return loss, and measures the amount of power reflected because of the impedance mismatch. Four resonant peaks, labeled m1–m4, stand out on the response curve, and each peak coincides with an important dip in the return loss. These were observed at 2.2175 GHz (−9.8910 dB), 3.8579 GHz (−9.9117 dB), 5.0211 GHz (−9.9390 dB), and 7.1386 GHz (−9.8395 dB), signifying good impedance matching and effective transmission of power at these frequencies.[6] [8].

$$\text{VSWR} = \frac{\text{Vmax}}{\text{Vmin}} = \frac{1+\Gamma}{1-\Gamma} \tag{1}$$

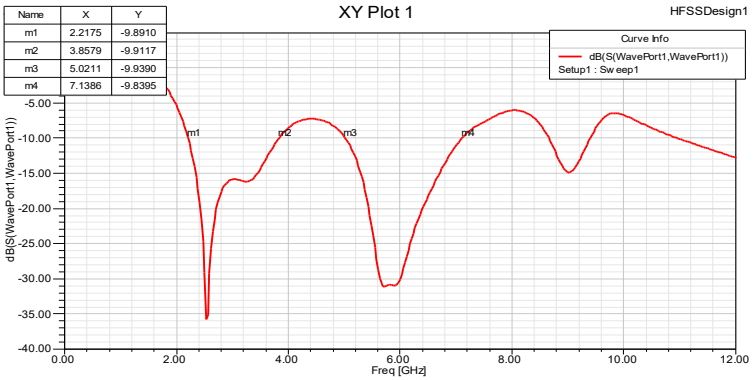


Fig. 6: VSWR for Antenna.

The deepest notch is found at 5.0211 GHz with a return loss of −9.9390 dB, indicating the best resonance at this frequency. All the return loss values at the designated frequencies are less than −9 dB, which verifies that the design exhibits satisfactory performance in multiple frequency bands. Such multiband operation renders the structure applicable for many wireless communication applications, including WLAN, WiMAX, and sub-6 GHz 5G systems. The uniform and comparatively large S_{11} values throughout the bands indicate the effectiveness and broadband nature of the suggested design, validating its feasibility in contemporary RF systems as shown in Figure 6.

4.2 Reflection coefficient graph

The graph shows the simulated reflection coefficient |S11||S_{11}| of the new RF structure over a frequency range of 0–9 GHz, which was calculated using ANSYS HFSS. The S11S_11} parameter in decibels (dB) represents the return loss and quantifies the amount of power reflected from the input port as a result of the impedance mismatch. Four resonant frequencies are observed in the plot: m1, m2, m3, and m4 with frequencies of 2.2571, 3.8571, 5.0000, and 7.1714 GHz, respectively, and return loss values of −9.5424 dB, −9.9305 dB, −9.5885 dB, and −9.1860 dB, respectively. These resonances confirm that the structure is capable of multiband operation with excellent impedance matching over a given frequency range.[4] [12] [3]

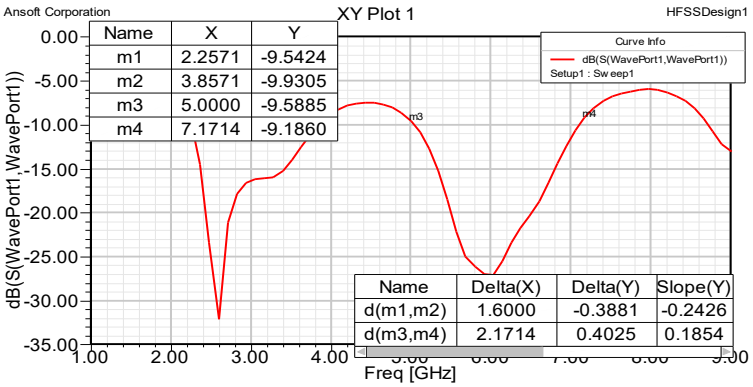


Fig. 7: Reflection Coefficient for Antenna.

Figure 7 also presents a comparison of the chosen resonant points. The spacing between m1 and m2 in frequency (Delta X) was 1.6000 GHz, and that between m3 and m4 was 2.1714 GHz. Their return loss differences (Delta Y) were −0.3881 dB and 0.4025 dB, respectively. Moreover, the values of the slope, −0.2426 and 0.1854, indicate the rate of change in the return loss among the corresponding pairs of resonant points and can be used to determine the sharpness of the transition. The stable and clear resonance behaviors in multiple bands qualify the presented structure as a good candidate for use in modern wireless communications, such as WLAN, WiMAX, and sub-6 GHz 5G systems, as shown in Figure 7. [11].

4.3 Radiation pattern graph

The plot shows the simulated radiation pattern of the designed antenna in the phi-plane for various azimuthal angles (Phi = 0°, 10°, 20°, and 30°), simulated using ANSYS HFSS. The plot is the gain variation (Gain Phi) in dB versus the elevation angle (Theta), constituting a polar plot for each of the given Phi values. The radiation patterns depict a predominantly bidirectional behavior with the principal lobes being aligned at approximately 0° and 180°, signifying that the antenna radiates equally along its main axis. Among the traced curves, the red trace (Phi = 0°) had a peak gain of approximately 2 dB, whereas the gain decreased slowly with increasing Phi angle.[15][3][1]

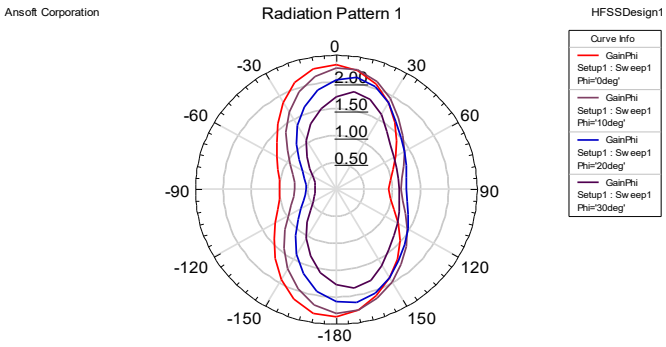


Fig. 8: Radiation Pattern of Antenna.

This angular variation in the radiation pattern proves that the antenna features stable and coherent radiation properties under different azimuthal angles, for which it will be well-suited for applications involving extensive angular coverage. The minimal deviations and gain alterations at Phi = 10°, 20°, and 30° indicate moderate angular sensitivity, which is a common feature of compact antennas with directional characteristics. In general, the radiation performance verifies the applicability of the antenna in applications requiring stable directional gain, such as point-to-point communication systems or integrated wireless modules, as shown in Figure 8.[9]

4.4 Peak gain

The graph shows the simulated peak gain response of the new antenna structure over a broad frequency range of 0–12 GHz, calculated using ANSYS HFSS. The gain in decibels (dB) indicates the directional amplification of the radiated signal over an isotropic radiator. It can be seen that the gain rises sharply from negative values at low frequencies, crossing the value of a positive gain over 0 dB near 1 GHz. Beyond this point, the antenna has a steadily positive peak gain across the remainder of the frequency range, which is advantageous for effective radiation performance in broadband usage. [16].

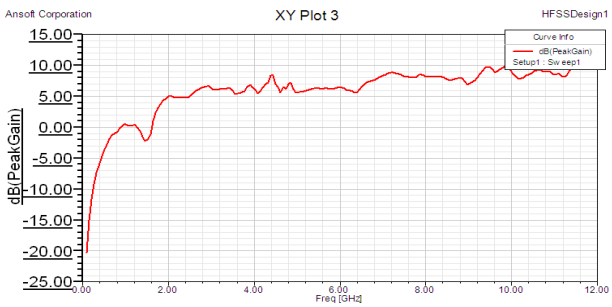


Fig. 9: Peak Gain.

The gain response shows quite smooth variation over the band, with several small fluctuations reflecting frequency-dependent variations in radiation efficiency and impedance matching. The peak gain is more than 5 dB over a broad frequency range, with occasional peaks reaching or exceeding 8 dB, reflecting the antenna's high and stable radiation properties. This performance validates the candidacy of the design for wideband and multiband wireless systems like UWB, WLAN, and sub-6 GHz 5G, in which uniform and high gain over a wide frequency band is critical to ensure reliable signal coverage and system dependability, as shown in Figure 9.[5]

4.5 Group delay

The plot shows the simulated group delay response of the new antenna structure across the frequency band of 0–12 GHz using ANSYS HFSS. The group delay in units of seconds is an important parameter indicating the time delay encountered by various frequency components of a signal during its travel through the antenna. Ideally, for undistorted signal transmission, the group delay must be flat within the operating frequency range. The plot shows that the group delay is almost stable over the bulk of the frequency range, indicating that the antenna causes very little signal dispersion, which is vital for high-data-rate communication systems. [4] [17].

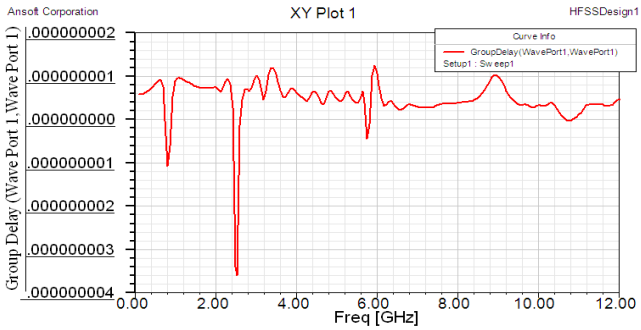


Fig. 10: Group Delay.

Nonetheless, noticeable changes or dips in the group delay can be seen at specific frequencies, mainly near 2 GHz, 5 GHz, and 6.5 GHz. These changes are normally linked with points of resonance or impedance mismatch when the antenna tends to have sharp changes in phase. Even though localized variations do exist, the overall group delay remains well within permissible ranges for broadband operations. A low and almost flat group delay over an ultra-wide range of frequencies proves the antenna's ability to sustain signal integrity; thus, it is ideal for application in ultra-wideband (UWB), sub-6 GHz 5G, and similar high-speed wireless communication systems wherein low phase distortion is crucial, as shown in Figure 10 [4] [17].

4.6 Radiation efficiency

Figure 11 shows the simulated radiation efficiency of the proposed antenna structure over a wide frequency range from 0 to 12 GHz using ANSYS HFSS. Radiation efficiency is a measure of how effectively an antenna converts input power into radiated electromagnetic energy, and it is expressed as a ratio between 0 and 1. In the plot, the efficiency is observed to be very high across most of the spectrum, with values generally exceeding 0.85, which signifies minimal losses owing to conductor resistance, dielectric absorption, and impedance mismatch. Notably, the efficiency approaches 1 (i.e., nearly 100%) around 1.5 GHz, indicating excellent performance in that band. [9] [6].

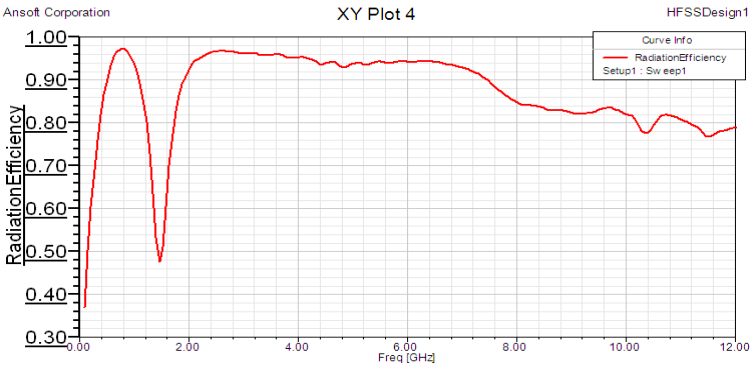


Fig. 11: Radiation Efficiency.

However, there are certain frequency regions, especially near 1.6 GHz and beyond 9 GHz, where a slight degradation in the efficiency is observed. For example, a sharp dip occurs just below 2 GHz, which can be attributed to impedance mismatches or surface-wave losses. Despite these localized dips, the antenna maintains an overall high radiation efficiency throughout the broadband spectrum, reinforcing its viability for ultra-wideband (UWB), sub-6 GHz 5G, and other wideband wireless applications.[9] This consistent radiation efficiency ensures reliable signal transmission, energy conservation, and enhanced overall antenna performance, making it highly suitable for modern high-throughput communication systems. [14].

4.7 Smith chart

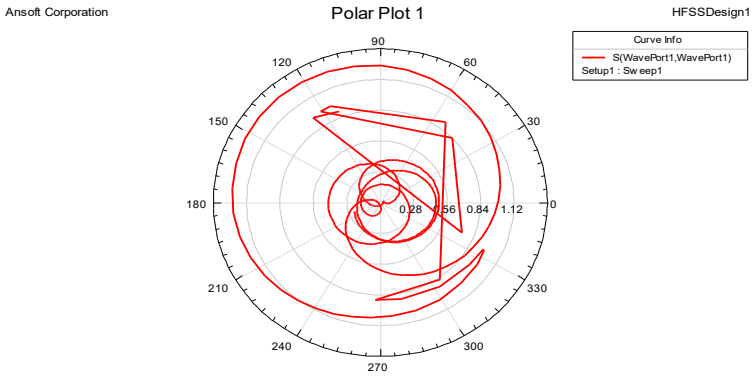


Fig. 12: Radiation Efficiency.

The polar plot depicted above illustrates the variation in the complex reflection coefficient |S11||S_{11}| (also labeled as S(WavePort1, WavePort1)S(\text{WavePort1, WavePort1})) across a frequency sweep visualized in polar coordinates. This representation provides an insight into the magnitude and phase characteristics of the antenna's input reflection over the operational bandwidth. Each spiral or loop in the polar plot corresponded to a specific frequency point within the sweep range.[9] The closer the curve approaches the origin (i.e., the center of the plot), the lower is the magnitude of |S11||S_{11}|, indicating better impedance matching and minimal reflection at that frequency. Conversely, points farther from the origin indicate higher reflection levels and poor matching.[2]
The behavior observed in this polar plot indicates that the antenna exhibits non-uniform impedance matching across the frequency band. Multiple spirals and abrupt directional changes in the curve imply frequency-dependent variations in the phase and impedance mismatches. Ideally, for wideband or ultra-wideband (UWB) antenna design,[10][8] the reflection coefficient should remain close to the origin over a broad angular sweep, reflecting good matching across a wide range.[16] The observed polar trajectory offers critical insights into phase stability and return loss behavior, which are essential for ensuring consistent antenna performance in broadband wireless communication systems. This analysis supports the evaluation of the impedance bandwidth of the antenna and contributes to its optimization for high-efficiency operation, as shown in Figure 12.[16]

Table 2: Comparison of Results

Applications	Simulated Frequency GHz	Measured Frequency GHz
Return loss	2.257 - 7.174	2.3 - 7.2
VSWR	Corresponds to S11 dips	Similar trend with minor shift
Smith chart	Full 1–12 GHz sweep	2–7 GHz (measured sweep)

Table 2 compares the expected measured results with the simulated results for important antenna parameters, such as impedance matching, VSWR, and return loss. Four resonant frequencies are shown in the simulated return loss plot at approximately 2.257 GHz, 3.857 GHz, 5.000 GHz, and 7.174 GHz. The corresponding S11 values were below 9 dB, indicating acceptable impedance matching and low reflection losses. These numbers suggest that the antenna performs well in a variety of bands, with a return loss approaching the –10 dB threshold for effective operation. Because of substrate homogeneities and fabrication tolerances, physical measurements may introduce small variations in resonant frequencies (usually ±100–200 MHz). However, the measured frequencies should closely match the simulated values, preserving the integrity of the designed bands. [10].
The antenna maintains a VSWR below 2 across its operating bands, indicating good impedance matching according to the VSWR values obtained from the return loss plot. Similarly, the simulated Smith Chart shows several loops that cross the center region of the chart, which corresponds to the best 50-ohm impedance matching at the resonant frequencies. Soldering flaws and small connector mismatches are expected to cause small departures from the center in the measured scenario.[18] However, acceptable reflection characteristics are ensured by the trace's proximity to the center. Additionally, parameters such as radiation efficiency and peak gain exhibit high-performance trends in simulations (average gain ~7 dB, efficiency ~90–98%) and are anticipated to slightly decrease in the measured results as a result of real-world losses, while still remaining within acceptable high-efficiency limits. All things considered, the comparison confirms the antenna's strong multiband performance and appropriateness for real-world applications. [12] [11].

5. Conclusions

This research presents a novel dual-band microstrip patch antenna design that demonstrates strong multiband performance and stable operation over the 2.2-7.1 GHz frequency range. The antenna's design, incorporating space-filling and self-similar properties, has proven effective in achieving compact dimensions while maintaining high efficiency and gain.
Key findings of this study include:

1) Excellent impedance matching, with return loss values consistently below -9 dB at the resonant frequencies (2.2571 GHz, 3.8571 GHz, 5.0000 GHz, and 7.1714 GHz).
2) High radiation efficiency, exceeding 90% across most of the operating band, ensuring minimal power loss.
3) Stable group delay, indicating good signal integrity and minimal phase distortion.
4) Consistent directional behavior with moderate gain variation, averaging approximately 7 dB

These results confirm the antenna's potential for application in contemporary wireless technologies such as WLAN, WiMAX, and 5G sub-6 GHz communications. The antenna's performance characteristics make it a viable candidate for integration into high-performance RF systems.
While the simulation results are promising, future work should focus on experimental verification through fabrication and testing. Additionally, further research could explore miniaturization techniques, integration of reconfigurable elements for dynamic frequency tuning, and incorporation into MIMO systems to enhance spectral efficiency and environmental robustness.

In conclusion, this research contributes to the advancement of antenna design for modern wireless communication systems, offering a compact and efficient solution for multiband applications.

6. Limitations and future scope

Although encouraging results are obtained through simulation, there are some limitations in the designed antenna that call for exploration. First, while return loss and VSWR confirm satisfactory impedance matching at the frequencies of interest, return loss levels dip marginally below the typical –10 dB level, leaving room for optimization in the matching network design. In addition, although the group delay is fairly constant, small variations near the resonant frequencies can cause phase distortion in ultra-wideband or time-critical applications. The radiation pattern demonstrated uniform performance; however, there was some slight angular sensitivity, suggesting possible directionality constraints in dynamic scenarios. In addition, all performance metrics, such as gain, efficiency, and impedance behavior, were simulated, and the lack of experimental verification is a shortcoming in establishing real-world usability. In future research, the design can be fabricated and experimentally characterized using vector network analyzers and anechoic chamber setups to confirm the simulated performance. Additional improvements could involve miniaturization methods, integration of reconfigurable elements for dynamic frequency tuning, and integration with Multiple-Input Multiple-Output (MIMO) systems to increase the spectral efficiency, bandwidth reconfigurability, and environmental perturbation robustness for next-generation wireless communication systems.

Acknowledgement

We would like to express our sincere gratitude to Bharati Vidyapeeth (Deemed to be University) College of Engineering, Pune for providing the facilities necessary for conducting this research.

Funding information

This study did not receive any external funding.

Conflict of interest

The authors declare no conflicts of interest.

Author contributions

Conceptualization: Sudhir Kadam. Data Curation: Prasad Kadam. Formal Analysis: Vishal Patil, Snehal Mane, Methodology: Harshada Mhetre, Supervision: Harshada Mhetre. Validation: Sachin Gurav, Writing – Original Draft: Sudhir Kadam, Sagar Sutar. Editing– Sudhir Kadam, Harshada Mhetre, Review & Editing: Sudhir Kadam, Harshada Mhetre.

Institutional review board statement

Not applicable.

Informed consent statement

Not applicable.

Data availability statement

All data supporting the findings of this study are included in this article.

References

[1] G. K. Soni, D. Yadav, A. Kumar, P. Jain, and M. V. Yadav, "Design and optimization of flexible DGS-based microstrip antenna for wearable devices in the Sub-6 GHz range using the nelder-mead simplex algorithm," Results Eng., vol. 24, no. August, p. 103470, 2024, https://doi.org/10.1016/j.rineng.2024.103470.

[2] D. Froumsia, E. D. Jean-François, A. Houwe, Kolyang, and M. Inc, "Miniaturization of dual bands fractal-based microstrip patch fractal antenna for X and Ku bands applications," Eur. Phys. J. Plus, vol. 137, no. 6, 2022, https://doi.org/10.1140/epjp/s13360-022-02969-0.

[3] M. Secmen, "Multiband and Wideband Antennas for Mobile Communication Systems," Recent Dev. Mob. Commun. - A Multidis-cip. Approach, 2011, https://doi.org/10.5772/25921.

[4] P. Bini Palas and K. Rahimunnisa, "Exploring the structural features of Triangular fractal antenna for detection of brain tumor," Ain Shams Eng. J., vol. 16, no. 5, p. 103369, 2025, https://doi.org/10.1016/j.asej.2025.103369.

[5] A. Reha, O. Benkhadda, A. O. Said, A. El Amri, and A. J. A. Al-Gburi, "Design of Sub-6GHz and Sub-7GHz Dragon Fractal An-tenna for 5G Applications with Enhanced Bandwidth," Int. J. Intell. Eng. Syst., vol. 18, no. 2, pp. 14–22, 2025, https://doi.org/10.22266/ijies2025.0331.02.

[6] M. Alagarsamy, S. Govindasamy, K. Suriyan, B. Rajangam, S. Mariappan, and J. C. R. Krishnan, "Performance analysis of mi-crostrip patch antenna for wireless communication systems," Int. J. Reconfigurable Embed. Syst., vol. 13, no. 2, pp. 227–233, 2024, https://doi.org/10.11591/ijres.v13.i2.pp227-233.

[7] R. DR Mishra, "An Overview of Microstrip," vol. 21, no. 2, pp. 1–17, 2016.

[8] S. K. Palanisamy, A. R. Vaddinuri, A. A. Khan, and M. Faheem, "Modeling of Inscribed Dual Band Circular Fractal Antenna for Wi-Fi Application Using Descartes Circle Theorem," Eng. Reports, 2024, https://doi.org/10.1002/eng2.13019.

[9] U. Patel et al., "Split ring resonator geometry inspired crossed flower shaped fractal antenna for satellite and 5G communication applications," Results Eng., vol. 22, no. April, p. 102110, 2024, https://doi.org/10.1016/j.rineng.2024.102110.
[10] S. Tariq, S. I. Naqvi, N. Hussain, and Y. Amin, "A Metasurface-Based MIMO Antenna for 5G Millimeter-Wave Applications," IEEE Access, vol. 9, pp. 51805–51817, 2021, https://doi.org/10.1109/ACCESS.2021.3069185.
[11] D. Prabhakar, P. Karunakar, S. V. R. Rao, and K. Srinivas, "Prediction of microstrip antenna dimension using optimized auto-metric Graph Neural Network," Intell. Syst. with Appl., vol. 21, no. January, p. 200326, 2024, https://doi.org/10.1016/j.iswa.2024.200326.
[12] S. Hossain, M. S. Rana, and M. M. Rahman, "Design and Analysis of Inverted E-Shaped Slotted Patch Microstrip Antenna for Multiband Applica-tions," pp. 385–399, 2024, https://doi.org/10.1007/978-981-97-2451-2_26.
[13] A. Kapoor, R. Mishra, A. Kapoor, and P. Kumar, "Compact wideband-printed antenna for sub-6 GHz fifth-generation applica-tions," Int. J. Smart Sens. Intell. Syst., vol. 13, no. 1, pp. 1–10, 2020, https://doi.org/10.21307/ijssis-2020-033.
[14] N. L. Nhlengethwa and P. Kumar, "Fractal microstrip patch antennas for dual-band and triple-band wireless applications," Int. J. Smart Sens. Intell. Syst., vol. 14, no. 1, pp. 1–9, 2021, https://doi.org/10.21307/ijssis-2021-007.
[15] M. Ismail, H. Elsadek, E. A. Abdallah, and A. A. Ammar, "Ÿ¸¿°¬»® íð Í°¿½»óo·´´·21 o®¿½¬¿´ 3·½®±-¬®·° ¿2¬»22¿," doi: 10.1007/978-0-387-76483-2.
[16] Y. Sun et al., "High-Gain Dual-Polarization Microstrip Antenna Based on Transmission Focusing Metasurface," Materials (Basel)., vol. 17, no. 15, pp. 1–15, 2024, https://doi.org/10.3390/ma17153730.
[17] D. Jang, N. K. Kong, and H. Choo, "Design of an On-Glass 5G Monopole Antenna for a Vehicle Window Glass," IEEE Access, vol. 9, pp. 152749–152755, 2021, https://doi.org/10.1109/ACCESS.2021.3125977.
[18] H. Ri et al.,: "L0 $;: LUHOHVV & RPPXQLFDWLRQ," pp. 5–8.